

This is an Open Access document downloaded from ORCA, Cardiff University's institutional repository: <https://orca.cardiff.ac.uk/id/eprint/130113/>

This is the author's version of a work that was submitted to / accepted for publication.

Citation for final published version:

Chong, Cheng Tung, Chiong, Meng-Choung, Ng, Jo-Han, Tran, Manh-Vu, Valera-Medina, Agustin, Józsa, Viktor and Tian, Bo 2020. Dual-fuel operation of biodiesel and natural gas in a model gas turbine combustor. *Energy and Fuels* 34 (3), pp. 3788-3796. 10.1021/acs.energyfuels.9b04371

Publishers page: <http://dx.doi.org/10.1021/acs.energyfuels.9b04371>

Please note:

Changes made as a result of publishing processes such as copy-editing, formatting and page numbers may not be reflected in this version. For the definitive version of this publication, please refer to the published source. You are advised to consult the publisher's version if you wish to cite this paper.

This version is being made available in accordance with publisher policies. See <http://orca.cf.ac.uk/policies.html> for usage policies. Copyright and moral rights for publications made available in ORCA are retained by the copyright holders.



Dual-Fuel Operation of Biodiesel and Natural Gas in a Model Gas Turbine Combustor

Cheng Tung Chong^{a,*}, Meng-Choung Chiong^b, Jo-Han Ng^c, Manh-Vu Tran^d, Agustin Valera-Medina^e, Bo Tian^f

^a China-UK Low Carbon College, Shanghai Jiao Tong University, Lingang, Shanghai 201306, China.

^b School of Mechanical Engineering, Faculty of Engineering, Universiti Teknologi Malaysia, 81310 Skudai, Johor, Malaysia.

^c Faculty of Engineering and Physical Sciences, University of Southampton Malaysia (UoSM), 79200 Iskandar Puteri, Johor, Malaysia.

^d School of Engineering, Monash University Malaysia, Jalan Lagoon Selatan, 47500 Bandar Sunway, Selangor,

^e College of Physical Sciences and Engineering, Cardiff University, Wales, UK

^f Department of Engineering, University of Cambridge, Trumpington Street, CB2 1PZ Cambridge

Abstract

The dual-fuel combustion characteristics of palm biodiesel/methyl esters (PME) and natural gas (NG) in a model gas turbine swirl flame burner is investigated. The PME is atomised into a spray, while the gaseous NG is premixed with the main bulk swirling air before entering the combustion chamber. The fuels are supplied to the burner outlet at the PME:NG ratio of 90:10, 80:20 and 70:30 by mass. The preheated NG/air mixture flow passes through an axial swirler before mixing with the liquid fuel spray at the burner outlet for ignition. The dual-fuel flames are compared with the baseline single fuel operation at the same thermal power output to assess the flame spectroscopic and emissions characteristics. The dual-fuel PME/NG flame structure is similar to the PME, where the sooty flame brush is noticeably absent. The PME and PME/NG flames emit higher peak intensity of OH* and CH* radicals as compared to diesel at the same equivalence ratio. Dual fuel operation results in lower NO but higher CO at $\phi = 0.9$ as compared to pure diesel and PME spray flames. The higher CO emission level for dual-fuel is attributed to poor mixing and incomplete combustion as a result of reduced air flow. At leaner operation of $\phi = 0.65$, enhanced turbulence due to higher bulk air flow results in improved mixing, lowering the overall CO but increasing the NO emissions due to the more intense flame core. The study shows that optimisation of the multiphase dual-fuel injection system is needed to achieve low emissions in a gas turbine combustor.

Keywords: dual-fuel; biodiesel, gas turbine, multiphase injector, emissions, spectroscopy

*Corresponding author

Address: China-UK Low Carbon College, Shanghai Jiao Tong University, Lingang, Shanghai 201306, China

Email: ctchong@sjtu.edu.cn ; Phone: +(86)15026970243

1.0 Introduction

Global reliance on bioenergy has been on the rise since the last decade [1], primarily driven by worldwide decarbonising efforts, stringent emissions requirements and global anxiety on finite fossil fuels reserves [2]. Biodiesel is one of the biofuels that is widely adopted especially in the transportation sector, with a global annual production reaching 36 billion in 2016 and is projected to increase in the future [3]. The usage of biodiesel is envisaged to extend to stationary combustion system such as gas turbines to reduce the reliance on conventional fossil fuels, apart from achieving positive greenhouse gas reduction effect. This has led to the development of fuel-flexible combustor, which is not limited to only switching the operating fuel, but also the adaptation of multi-fuel injection system. This strategy allows the adoption of bio-derived fuels in conjunction with conventional fuel in the combustion system, while maintaining minimum or no modification to the combustion system.

The concept of dual-fuel operation has been extensively explored in internal combustion engine. By using natural gas as a supplemental fuel, Selim et al. [4] demonstrated that dual-fuel operation in a single cylinder Ricardo E6 indirect injection diesel engine resulted in higher in-cylinder pressure rise rate compared to conventional diesel engine with single fuel operation. Wannatong et al. [5] demonstrated that natural gas injection with constant pilot diesel supply increased the heat release rate and in-cylinder pressure in a diesel engine, but the ignition delay was found to significantly reduce. Similarly, Lounici et al. [6] showed that dual-fuel operation in engine resulted in the increase of in-cylinder pressure at high engine load. The shortcoming of dual-fuel operation can be overcome via the alteration of injection timing of natural gas to improve the combustion efficiency at low and partial loads [7,8]. Sun. et al. [9] proposed the increase of pilot diesel fuel and modification of injection timing for dual-fuel operation to increase the peak in-cylinder pressure and heat release rate. On emissions performance, Papagiannakis et al. [10] showed that dual-fuel operation of diesel and natural

gas reduced the NO_x emissions for low and high load, as natural gas promotes lean combustion that avoids the formation of local hotspot [15]. Some have argued that natural gas contains higher specific heat capacity that results in the reduction of flame temperature and subsequently lower NO_x emissions when operating in dual fuel mode. Further reduction in NO_x can be achieved by improving strategic control of engine parameters such as pilot fuel injection timing, temperature and pressure of intake charge [11].

It is envisaged that the concept of dual-fuel operation can be extended to stationary combustion system, such as the gas turbine system for power generation purpose. In fact, there has been some researchers investigating the combustion performance of dual-fuel operation under continuous swirl flame conditions, such as those conducted in a gas turbine combustor equipped with a radial swirler operating with biodiesel/natural gas [12]. It has been demonstrated that biodiesel/natural gas combustion resulted in higher NO than neat natural gas by an average of 10 ppm at fuel-lean conditions. Further, the dual-fuel combustion also led to higher CO than natural gas by roughly 60 ppm when compared under the same equivalence ratio. Researchers from Cardiff University [13] experimented the multiphase fuel combustion in a gas turbine combustor, via the use of methane/CO₂ blends with biodiesel and diesel as operating fuels. It was shown that the co-combustion of methane/CO₂ with waste cooking oil-derived biodiesel at 20 kW, coupled with 10% of CO₂ blend dilution reduced the CO emissions by approximately 87%. A reduction of NO_x emissions by 50% was also achieved with the fuel mixtures, owing to the lower flame temperature resulting from CO₂ dilution. It was concluded that the co-combustion strategy resulted in cleaner combustion with improved flame stability.

The concept of multiphase fuel combustion has been extended to accommodate biofuels that are of low calorific value in nature. Jiang and Agrawal [14] examined the combustion characteristics of methane-glycerol using a swirl flame burner equipped with flow-blurring atomisation technique. It was shown that the presence of methane promotes vaporisation of

glycerol, resulting in enhanced oxidation rate with near complete combustion in spite of the noticeable difference in flame structure. Neat glycerol combustion exhibited lower NO emissions than dual-fuel combustion owing to lower flame temperature, but the latter produced lower CO emissions. Another glycerol combustion study conducted by Queiros et al. [15] employed the concept of multiphase atomisation technique. The glycerol is injected into the combustor as spray assisted by an air-assist atomiser. The fuel vapour is mixed with natural gas and hydrogen to form a combustible mixture for burning. Post-combustion products were quantified and the deposits on the combustion chamber walls were analysed. It was reported that the increase in glycerol proportion resulted in more deposit formation at the burner exit. The deposits consisted of trace elements such as Na, K and Cl, which could undesirably shorten the life-span of the critical components such as turbine blades. The emissions of NO from glycerol/natural gas/hydrogen combustion were consistently lower than neat natural gas by an average of 10 ppm for the range of atomising air-fuel at 0.5-2, but the CO emissions were noticeably higher when the atomiser air-fuel ratio was 0.5.

Natural gas is known to exhibit relatively clean combustion characteristics compared to other types of fossil fuels [16][17]. By using natural gas as a supplemental fuel and palm biodiesel/methyl esters (PME) as main pilot fuel spray, the present study investigates the dual-fuel combustion characteristics in a lab-based axial swirl model gas turbine burner. This study focuses on the global flame structure, quantifies the combustion intermediate species via spectroscopic approach and investigates post-combustion emissions characteristics of the PME/NG swirl flames at different equivalence ratios. The potential of PME/NG dual fuel combustion under swirling flame condition is assessed, by comparing with the performance of baseline single fuel, i.e. pure diesel and PME reacting swirl flames.

2.0 Experimental

2.1 Swirl Burner System

The reacting swirl flames in the present experiment is established under atmospheric condition using an axial swirl liquid spray flame burner. The schematic of the experimental setup is depicted in Fig. 1. Delivery of liquid fuel to the spray atomiser is accomplished by using a peristaltic pump (Longer BQ50-1J), coupled with a chamber that serves as a flow damper. Silicone tube with an inner diameter of 4 mm is used to transfer the liquid fuel from the fuel supply tank to the atomiser via a pump. An airblast-type atomiser (Delavan: SN type-30610-1) is employed to atomise the liquid fuel via prompt atomisation that occurs at the atomiser outlet. The atomising air and fuel orifice diameter are 1.73 and 0.5 mm, respectively. The atomisation characteristics of the injector is detailed in [18]. The atomiser is placed concentrically with an axial swirler that consists of six straight vanes tilted at 45° and mounted flush at the burner outlet. The geometric swirl number of the burner is approximated as 0.84, which provides a sufficiently strong swirl that is vital for flame stabilisation [19].

The swirling air flow in the combustor is generated as the main air passes through the angled axial swirler, subsequently mixes with the liquid fuel spray to form a combustible mixture. Fuel-air mixing is promoted by the recirculating turbulent flow which results in enhanced flame stabilisation. Preheating of the main air is carried out by using three rope heaters (Omega: FGR-100–240V, 500 W/rope) prior to flowing through the swirler. The air heating process is regulated by a PID heat controller system, monitored by a K-type thermocouple (1.5 mm diameter) positioned at 10 mm upstream from the burner outlet. Heat loss is minimised by insulating the burner wall with ceramic wool. The mass flow of main air and atomising air are regulated using Sierra SmartTrak 50 (accuracy: $\pm 1.5\%$ full scale) mass flow controllers. The supply of natural gas to the burner plenum is regulated using a flow meter.

The natural gas is premixed with preheated main air at the plenum before mixing with the liquid fuel vapour at the burner outlet. Fig 1b illustrates the multi-fuel injection system.

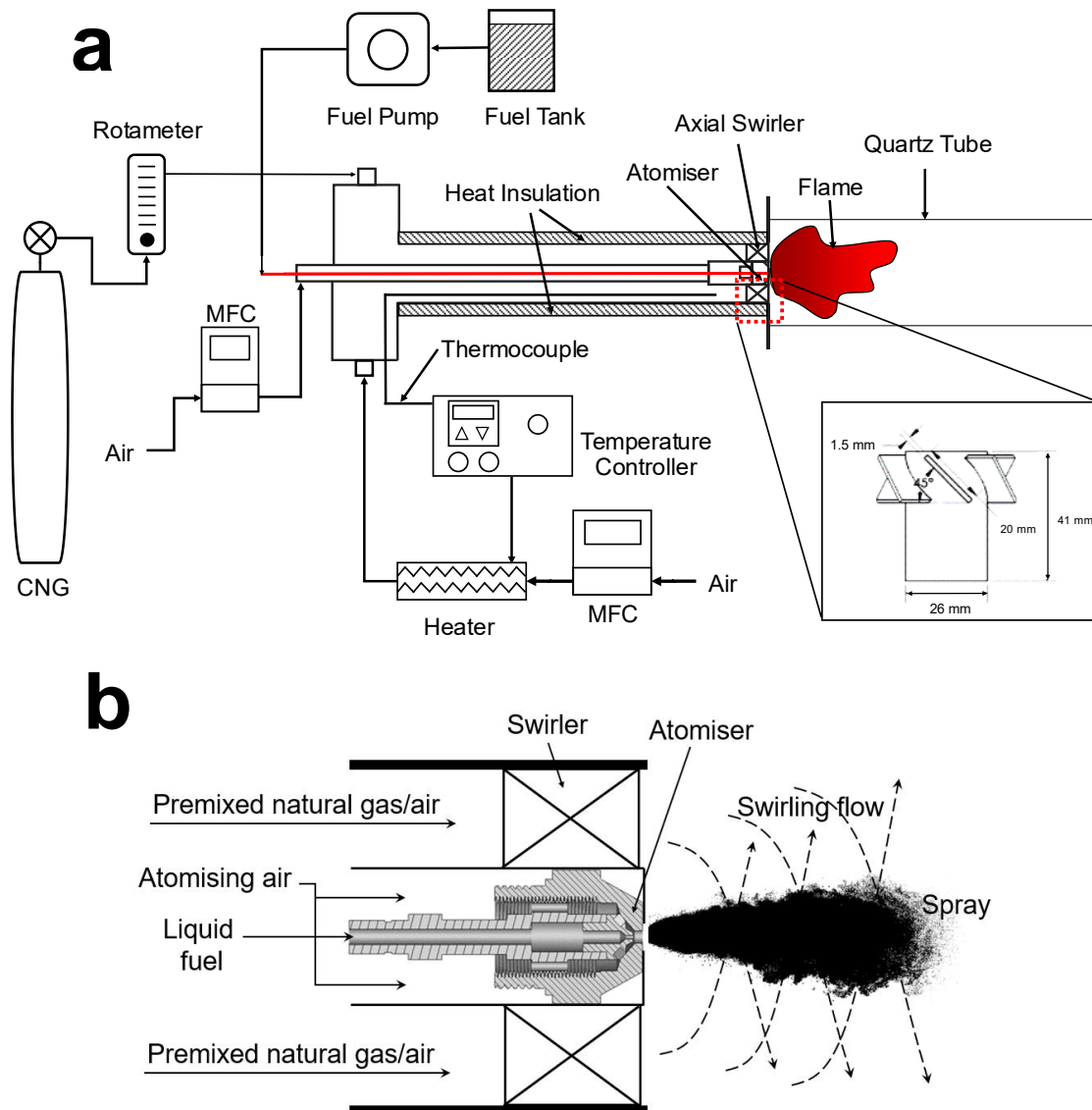


Fig. 1 Schematic of the (a) burner and flow delivery system and (b) multiphase fuel injection mechanism

2.2 Fuel preparation and properties

The fuels tested in this experiment are diesel, palm biodiesel (PME) and natural gas (NG). Diesel is purchased from a local petrol station. The palm biodiesel is produced in-house via the transesterification process, in which the palm-based cooking oil reacted with methanol and potassium hydroxide (KOH) at the at mass ratio of 114:50:1 (palm oil:methanol:KOH) to

produce the methyl esters. A magnetic stirrer is used to ensure thorough blending at constant temperature of 60 °C for 2 hours. The mixture is left overnight to allow separation into biodiesel and glycerol layers. The biodiesel is extracted and heated at constant temperature of 120 °C for 4 hours to vaporise the water and methanol. Characterisation of the PME is carried out using a gas chromatography (Agilent 7820A), which indicates the approximated composition as 66.3% methyl linoleic (18:2), 21.7% methyl oleic (18:1), 6.4% methyl palmitic (16:0) and 3.6% methyl stearic (18:0) by mass. The natural gas is supplied from a 20 MPa compressed natural gas tank and regulated via a flow meter.

Comparison of the fuel properties is shown in Table 1. PME is oxygenated and possesses lower heating value than biodiesel by approximately 12% on a mass basis. The viscosity and density for biodiesel is slightly higher than diesel. The molecular weight for the PME and diesel are approximated as 296.5 g/mol and 226 g/mol respectively. Natural gas is in gaseous form and contains the highest heating value per mass basis among the fuel tested. Natural gas consists of predominantly methane (86–96%) [20], hence for simplicity, the molecular weight of natural gas is approximated as methane for the calculation of the fuel/air ratio [21].

Table 1 Physiochemical properties for diesel, palm biodiesel and natural gas [21,22]

Properties	Unit	Diesel	PME	NG
Lower heating value	[MJ/kg]	42.57	37.4	45.0
Density	[kg/m ³]	843.27	867.7	0.8
Cetane Number	[-]	50	62.0	-
Octane Number	[-]	-	-	120
Kinematic Viscosity (40°C)	[mm ² /s]	2.40	4.6	-
AFR (Stoichiometric)	[-]	14.59	12.36	17.25

2.3 Measurement techniques

Imaging of the swirl flame appearance was performed using a digital camera (Canon EOS 600D) through an optically accessible quartz tube. The focal length and exposure time of the camera were set to 4 mm and 1/15 s, respectively. The flame images provide a qualitative comparison of the macro flame structure established from different fuels. The flame spectral emissions characteristics of the flames are investigated using a spectrometer (Avaspec-UL2048 Starline). The flame spectra are resolved spectrally that spans across the ultraviolet to near infrared range (200–900 nm). The light intensity is collected via the spectrometer slit with a width of 10 μm at the resolution of 0.1 nm, imaged onto the charged-coupled device (CCD) detector of 2048 pixels at the integration time of 1 s. The focal length of the slit from the flame is about 1 m. The signal-to-noise of the probe is >10 .

The concentration of the post-combustion exhaust gas pollutants was quantitatively measured using a gas analyser (KANE Quintox 9106). Among the measured gases include nitric oxide (NO), carbon monoxide (CO), carbon dioxide (CO₂) and oxygen (O₂) in the flue gas. The accuracy of the equipment was cross-checked using calibration gases prior to measurement. The sampling probe was positioned 13 mm from the exit plane of the combustor outlet, directly facing the flame to sample at the rate of 2 L/min via the sampling tube of 5 mm in diameter. Emissions sampling was performed at 5 equally spaced radial direction. The obtained data is used to derive the global emission value using the area-velocity weighted averaging method. The specifications of the measurement instruments are shown in Table 2.

Table 2 Specifications of measurement instruments

Analysis	Sensor/ Instrument	Range	Resolution	Uncertainty	Propagated Error
Flame spectra	Spectrometer	200-1000 nm	0.1 nm	± 0.1 nm	$\pm 1.3\%$
Post- combustion gas	Gas analyser	0-4000	1 ppm	<100 ppm; ± 5	$\pm 16.0\%$
	CO	ppm		ppm >100 ppm; $\pm 5\%$	
	NO	0-5000 ppm	1 ppm	<100 ppm; ± 5	$\pm 7.5\%$
				ppm >>100 ppm; $\pm 5\%$	
	CO ₂	0-20%	0.1 %	$\pm 5.0\%$ of reading	$\pm 4.2\%$
	O ₂	0-30%	0.01%	$\pm 0.2\%$	$\pm 1.3\%$

2.4 Operating conditions

The operating fuels used in the study are diesel, PME, NG and dual-fuel PME/NG of 90/10, 80/20 and 70/30 by mass. Fossil diesel and PME are chosen as baseline in this study. All flames are established under the constant thermal output power of 9.3 kW. Table 3 shows the operating conditions for the multiphase fuel injection at global equivalence ratio of $\phi = 0.65$. For liquid fuel injection, atomisation of the fuel is achieved by setting the atomising air-to-liquid ratio to 2.5. The mixture of the dense spray and atomising air created a locally vapour-rich mixture with equivalence of $\phi_L = 6-7$. The main air flow in the main annulus is preheated to 250 °C and premixed with natural gas at the burner plenum to form an ultra-lean conditions of $\phi_G < 0.3$. The swirling air/fuel mixture is injected into the combustor via a swirler, creating a strong swirl that enhances the mixing between liquid vapour and gaseous fuel, forming a globally lean mixture. The global equivalence ratio of the flames is varied between $\phi = 0.65-0.90$ by regulating the main air flow supply.

Table 3 Operating conditions for multi-fuel injection to form a globally lean mixture of $\phi = 0.65$

Fuel	Liquid phase				Gaseous phase		
	Fuel flow rate (g/s)	Atomising air mass flow rate (g/s)	ALR	ϕ_L	NG flow rate (g/s)	Main air mass flow rate (g/s)	ϕ_G
*Diesel	0.22	0.54	2.50	7.40	-	4.41	-
*PME	0.24	0.61	2.50	6.20	-	4.03	-
**NG	-	-	-	-	0.21	5.47	0.65
PME/NG 90/10	0.23	0.57	2.50	6.35	0.02	4.21	0.07
PME/NG 80/20	0.19	0.48	2.50	6.35	0.04	4.15	0.18
PME/NG 70/30	0.17	0.42	2.50	6.35	0.06	4.11	0.27

*Liquid fuel operation

** Gaseous fuel operation

3.0 Result and discussion

3.1 Global flame appearance

The swirl flames of diesel, PME, NG and PME/NG established at globally lean $\phi = 0.65$ and atmospheric condition are shown in Fig. 2. The continuous stable flames were established with the swirling air temperature preheated to 250 °C, while the liquid fuel atomisation was achieved by fixing the ALR at 2.5. In general, single fuel flames exhibit a flame appearance that is visibly different from the dual-fuel flames. For single fuel liquid spray flame, the generated spray forms a well-defined cone shape, assisted by the shear from swirling flow to enhance mixing. Diesel flame shows a yellowish flame brush owing to the formation of soot, as opposed to the PME flame that shows a clean bluish flame. Diesel is known to produce highly sooty flame due to the presence of aromatics, whereas PME spray flame is known to be soot-free, as shown in previous work [23]. The well-mixed gaseous natural gas flame stabilised at the swirler vane edges instead of anchoring at the central atomiser hub region. The flame was observed to be bluish, clean and stable, without any intermittent flicker of sooty flame brush.

A combination of the gaseous and liquid fuel results in a different flame structure, i.e. a hybrid structure that integrates the characteristic of a premixed gaseous flame and partially premixed vapor flame. The flame core where intense reaction happens is observed to be shorter and more compact. Occasional flickers of yellowish flame brush were observed which could be attributed to the pockets of fuel vapour that is incompletely burnt, presumably due to the swirl flow that recirculates some of the larger droplets back to the inner core. An increase of the NG fraction in the flame results in the reduced flame core intensity. The addition of NG increases the local equivalence ratio of the gaseous fuel stream, coupled with the heat provided from preheating increases the possibility of the mixture to react and assist in combusting with the central fuel spray. This explains the reduced occurrence of sooty flame brush for 70/30 dual

fuel flame, while the overall bluish flame resembles more closely to the pure NG flame. Another observation is that the dual flames are seen to weakly anchored to the burner outlet, unlike those of single fuel flames. The neat NG flame is stabilised and anchored at the edges of the swirler edge at burner outlet, while the liquid spray flame is seen to anchor at the atomiser hub at the injector outlet. A flame that is lifted can be susceptible to blowout should there be a fluctuation in the flow. It is believed that the interactive effects of flow field and mixing between the gaseous and liquid vapour could be the reasons for the detached flame phenomenon. An increase in the NG fraction in dual fuel leads to a visibly more stable flame, as the flame root can clearly be seen attached to the burner.

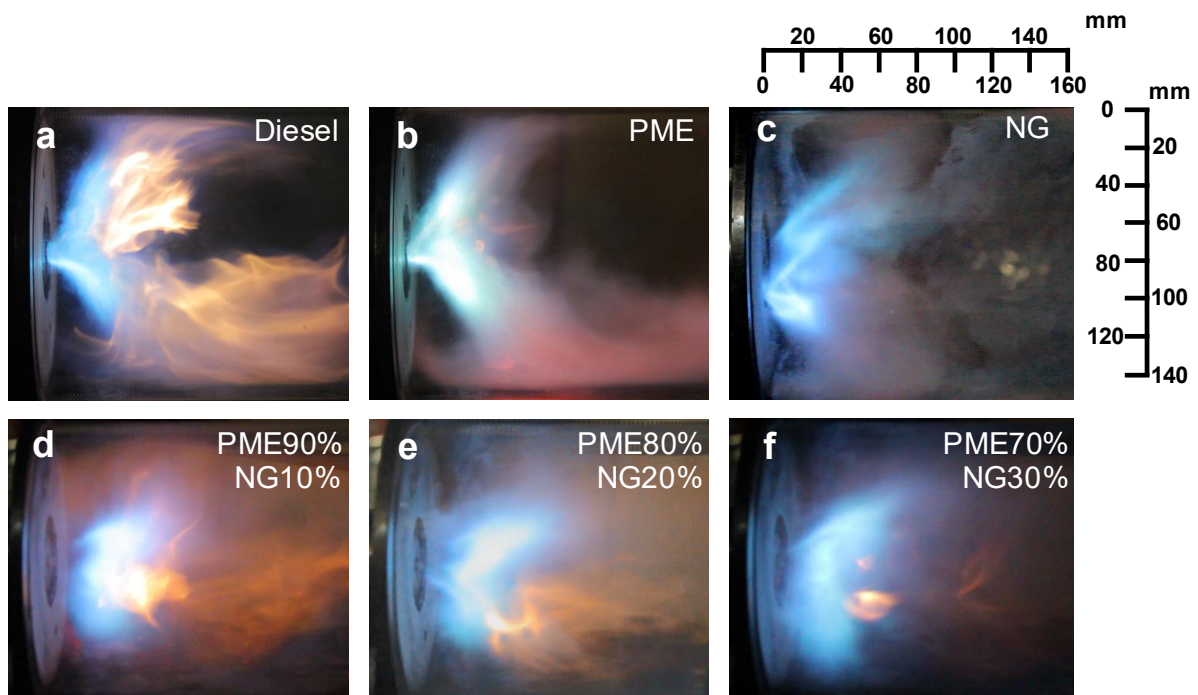


Fig. 2 Flame images for (a) diesel, (b) PME, (c) NG, (d) 90/10, (e) 80/20 and (f) 70/30 PME/NG at main swirl air temperature of 250 °C, ALR=2.5, $\phi = 0.65$.

3.2 Flame Spectroscopy

The flame spectra of diesel, PME, NG and PME/NG 80/20 swirl flames established at $\phi = 0.65$, ALR 2.5 are shown in Fig. 3. The spectra for PME, 80/20 PME/NG and NG are displaced by 5, 10, 15 nm respectively, relative to diesel to enhance clarity. Natural gas premixed with air, being a clean burning fuel, exhibits a relatively flat spectrum with minorly detected OH* radicals especially at lean-burning condition. The premixed flame emits near-zero soot and the flame reaction zones are not intense as the flame temperature is relatively low. The spectroscopic condition is starkly in contrast to those of liquid fuel flames. As the liquid fuel spray was injected into the combustion chamber, the mixture of atomising air and liquid vapour creates an ultra fuel-rich condition. Further mixing with the swirling air through strong shear flow and recirculation flow resulted in the dilution of spray, nonetheless the fuel vapour/air mixture is in partially premixed mode. Some larger droplets tend to burn off in diffusive nature, inadvertently contributing to the formation of soot. Diesel flame is known to be a heavily sooting owing to the presence of aromatics. The strong radiation from the soot results in the visibly yellowish flame brush downstream of the flame core. The flame core is where the strong shear flow between the swirling flow and the fuel vapour takes place, coupled with the premixed atomising air and fuel in the spray core, formed the highly mixed oxidiser and fuel vapour region that results in the bluish flame analogous to a premixed flame. The diesel flame spectrum shows a characteristic distinct broad sooty band ranging between 550 – 900 nm, which corresponds to the yellowish-orange flame brush as observed by naked eyes.

The PME swirl flame shows an intense bluish flame core with no sign of soot. This is reflected in the flame spectra where the soot band in the visible orange-yellow spectrum is not present. Instead, the intense radiative radicals of OH* and CH* are observed. PME is an inherently oxygenated molecule. The role of the oxygen in the methyl esters molecule acts as an oxidiser that promotes reaction, apart from suppressing the formation of soot. Soot

production is relatively low in biodiesel, as was concluded from many studies either in lab scale [23] or system level testings [24]. It is interesting to note that PME exhibits a distinct peak of 784 nm owing to the presence of trace element, i.e., potassium, which is the remnant from the catalyst (potassium hydroxide) used during the production stage. The dual-fuel PME/NG 80/20 exhibits a spectrum that is more biasly resembles PME, rather than the NG as evident by the visible peak of CH*. The PME/NG dual-flame shows a noticeably lower peak intensities of OH*, CN*, CH* and C₂* radicals compared to neat PME flame, which are represented by the peaks at 310, 388, 432, 515 nm respectively. Comparison of the spectra for dual-fuels at 90/10, 80/20 and 70/30 with baseline diesel flame is shown in Fig 4. The flame emission spectra for all dual-fuel are quite similar, except that the sooty band shows a gradual reduction in intensity as the NG fraction reduces from 30% to 10%. Natural gas, consisting of predominantly straight-chain alkane with trace inert gases, is not prone to the formation of soot similar to neat PME, as shown in Fig. 4b.

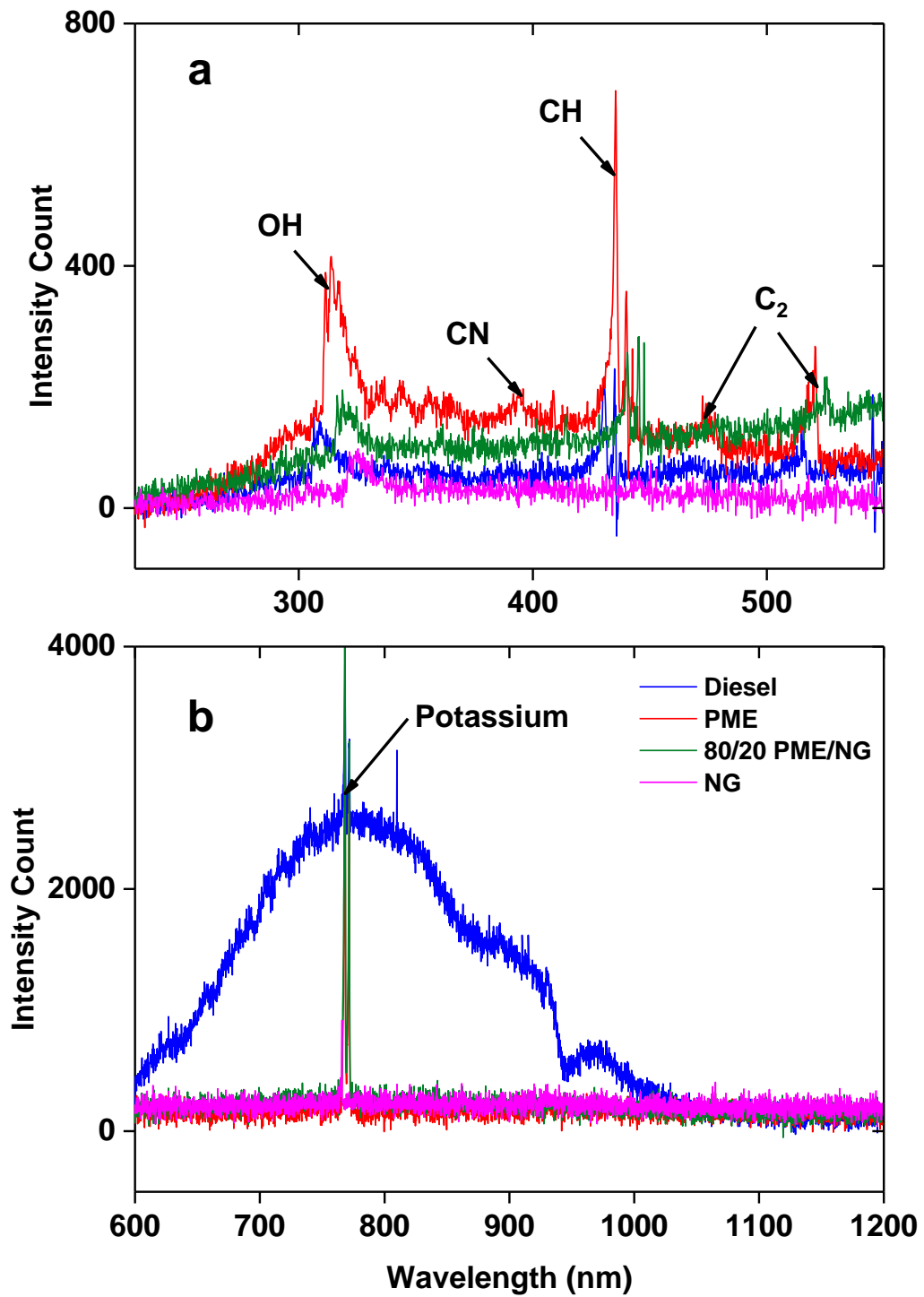


Fig. 3 Flame spectra (a) 200-600 nm (b) 600-1200 nm for diesel, PME and PME/NG dual fuel combustion at ALR 2.50, $\phi = 0.65$.

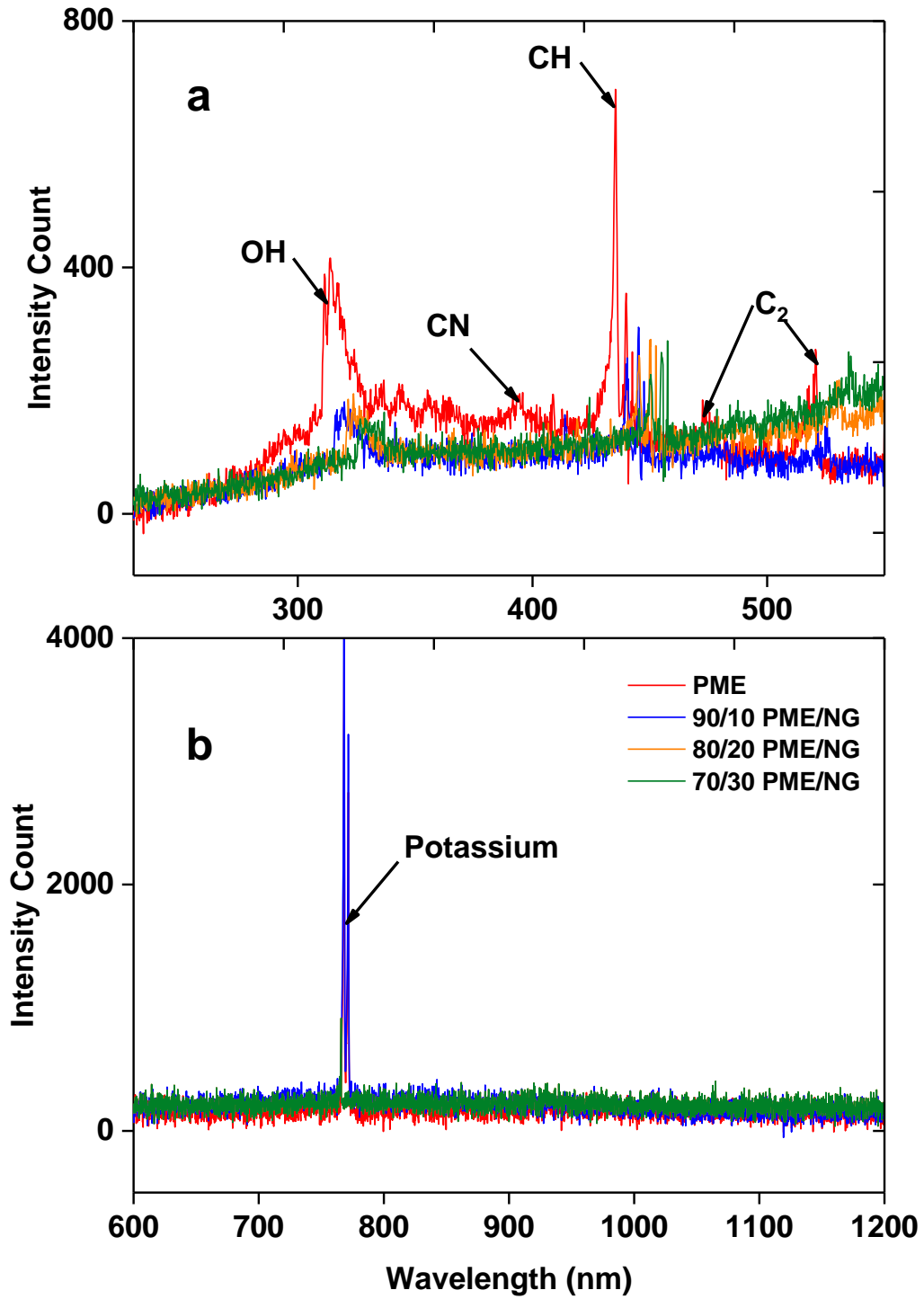


Fig. 4 Flame spectroscopy (a) 200-600 and (b) 600-1200 nm for diesel, and PME/NG dual fuel combustion at ALR 2.50 and $\phi = 0.65$.

Quantification of the radicals emitted from the flames is shown in Fig. 5. The spectral shows that lean swirl flames ($\phi = 0.65$) produced a reducing level of OH*, CH*, CN* and C₂* radicals as the fraction of NG increases from 0-30%. The peak intensity of the OH* and CH* radicals is reduced by a factor of 1.2 and 1.1 for 30% NG in PME compared to PME flame, indicating less heat release from the flame, conforming to the visual observation in which the flame becomes “weaker” and less intense. NG mainly consists of short chain of alkane, tends to produce insufficient H*, O*, OH* radicals compared to long chain hydrocarbons that are essential for the production of OH* and CH* radicals [25,26]. The formation of OH* is primarily from the CH + O₂ = CO + OH* reaction pathway. The intensity of the OH* radicals is known to correlate with flame temperature, such that higher flame temperature results in higher OH* intensity in the main reaction zone [27]. It is interesting to note that PME spray flame shows the highest intensity of OH* and CH*, whereas the diesel and blend show somewhat higher OH* and CH* intensity counts as compared to pure NG flame. The globally lean premixed flame presents the lowest OH* intensity owing to the low flame temperature, whereas those with liquid spray contains evaporating droplets that burns under near-stoichiometric mode, hence the OH* intensity is higher. The addition of short-chain NG also tends to reduce the O*, OH*, C*, CH* and CH₂*, thus the production of CN* and C₂* radicals is also reduced correspondingly [26,28,29]. For lean methane flame, the flame temperature is around 1500 K, hence the reaction pathway of CH₄ → CH₃ → C₂H₆ → C₂H₅ → C₂H₄ → C₂H₃ → C₂H₂ → CO becomes significant [30]. Acetylene (C₂H₂) that is produced from this pathway serves as one of the radicals that consumes CH radical via the reaction R1 [25]. Further, It has also been shown that methane plays a role in consuming the OH* radical via the reaction R2 [26]. These contribute to the lower OH* and CH* intensities in the NG-PME dual flames.



The lower volatility of PME droplets tends to have longer residence time in the flame and concentrates at the region of main reaction zone with significant droplet density [31,32]. This consequently increases the thickness of flame mean diffusive layer, resulting in intensified reactions that promotes the formation of combustion intermediate species [33–35]. However, the addition of NG results in the reactions taking place at a leaner mixture fraction region, in contrast to the non-premixed flame where reaction typically occurs at region with near stoichiometric mixture fraction [36]. The broadening of the reaction zone explains the reduction of C_2^* radical for NG-diluted mixtures, as the formation C_2^* radical is usually pronounced at locally fuel-rich reaction zone [29,37]. The reduction of the CN^* radicals in NG-mixed PME flame may be attributed to the combustion chemistry of lean flame. Formation of CN^* radical becomes significant when the flame temperature is higher than 2000 K [38] through reaction R3. The overall lean flame with lower flame temperature results in the oxidation of HCN^* radical to form NCO^* (Cyanato) or NH^* (Imidogen) radicals, via the reactions R4 and R5 [38], respectively. It has been shown in the work of [39] where the reactions R4 and R5 account for 66% and 34% of HCN oxidation, respectively, for flame with temperature below 2000 K. Thus, it is postulated that the globally lean flame of PME/NG dual flame suppresses the formation of CN^* radical.



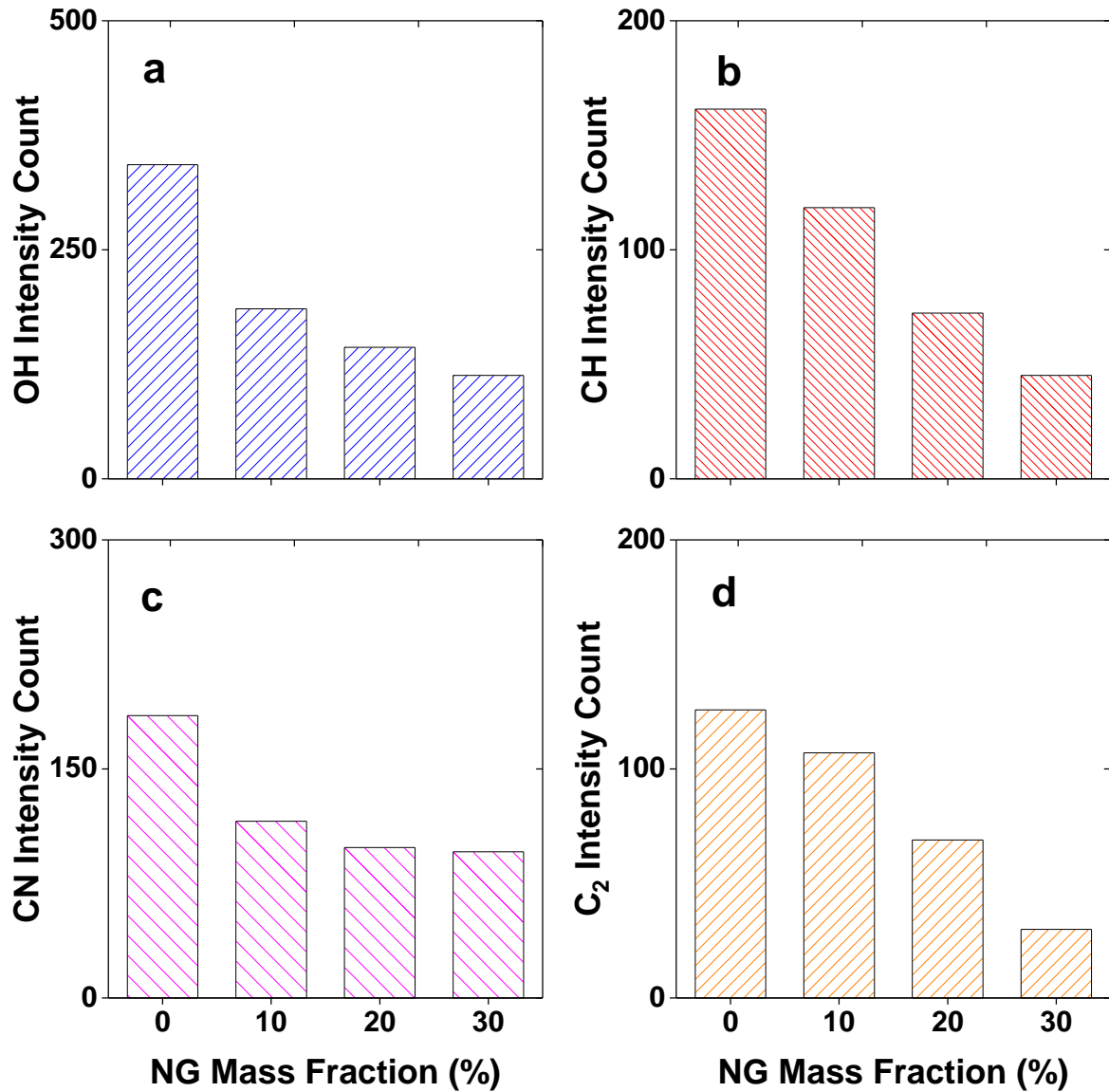


Fig. 5 The intensity counts of (a) OH (b) CH (c) CN (d) C_{2,470nm} radicals for PME with different NG mass fraction established at ALR=2.5, preheated swirl air temperature = 250 °C and $\phi = 0.65$.

5.0 Post-Combustion Emissions

5.1 Effect of Equivalence Ratio

Comparison of the post-combustion emissions of NO, CO, CO₂ and O₂ for flames established from dual-fuel PME/NG with pure diesel, PME and NG flames at different equivalence ratios is shown in Fig. 6. The flames were established at the fixed power output of 9.3 kW, ALR=2.5 with the main swirl air heated to 250 °C. Result shows that the dual-phase fuel injection of PME and NG does not necessarily lead to lower NO and CO emissions, partly in due to the inhomogeneity of mixture and incomplete mixing between the fuels and air. The case of PME/NG 90/10 shows considerable higher NO than neat PME and diesel flames between $\phi = 0.65-0.8$, as opposed to the lower NO emissions shown by the dual fuel case of PME/NG 70/30. Higher NO is prone to form at fuel-lean region for dual-fuels, but gradually decrease as the equivalence ratio approaches stoichiometric. This is counter-intuitive as conventional wisdom implies that flame temperature should be higher as the equivalence ratio approaches stoichiometric, thus higher NO should be produced. In the present work, we deduce that the inhomogeneity in the fuel mixture due to dual-fuel injection leads to the sharp rise in NO, which is supported by two observations: 1) the single fuel injection shows a rather flat profile of NO, indicating single fuel has a more homogenous mixing than dual-fuel injection, 2) the increase of CO emissions for dual-fuel with increasing equivalence ratio, which is indicative of incomplete combustion. The issue of mixing is closely related to the flow field inside the combustor

Dual fuel with NG fuel fraction at higher equivalence ratio shows a convergence of NO to a minimum level, while an opposite trend is shown for the CO emissions. As the main air flow decreases with increasing equivalence ratio, the mixing of NG with the main air flow becomes deficient, as pockets of unburnt mixture due to insufficient mixing and reduced swirl strength eventually led to the high level of CO emissions. From the combustor macro point of

view, the flow field plays a significant role in the pollutant formation. Under lean-burning condition, the main air flow entering the combustor is able to generate strong center toroidal recirculation flow, hence the unburnt product from the premixed air and NG can be effectively recirculated back to the flame to be burnt. This extends the residence time of the fuels in the combustor, enabling mixing to take place and subsequently react. Further, higher turbulence kinetic energy also reduces turbulence length scale, which in turn increases the higher turbulence energy dissipation rate that promotes mixing between fuels and air [35]. It is noted that the dual fuel of PME/NG 90/10 and 80/20 exhibit rather high NO at $\phi < 0.7$ compared to single fuel flames, but the value drops to a minima at $\phi = 0.85$. One plausible explanation is the incomplete mixing of fuel spray with the NG that results in the partial combustion of PME spray under fuel-rich condition, which forms a locally hot zone in the flame core that leads to high level of NO emissions. The mixing issue also becomes pertinent with the increase of equivalence ratio where the main swirling air is reduced, rendering insufficient strength of swirl flow that causes mixing to be impaired, subsequently leading to the production of CO during combustion. Further investigation on the flow field and flame structure is needed to yield better insight on their impact towards emissions.

The emissions of CO₂ are shown in Fig. 6c, where diesel, PME and NG exhibit a linear increasing trend of CO₂ with the increase of equivalence ratio. This is expected as more fuel is burnt and CO₂ is produced at higher equivalence ratio. PME exhibits consistently slightly higher CO₂ emissions than diesel and NG, owing to the oxygen molecules in the fuel that reacts into CO₂. However, the PME/NG dual flames exhibit a non-linear trend, indicating inconsistency in mixing and combustion. The PME/NG 90/10 case shows an increasing CO₂ emission up until $\phi = 0.8$, then followed by the onset of non-linearity due the effect of inhomogeneity of the fuel/air mixture. The dual-fuel case of PME/NG 80/20 and 70/30 show similar trend, albeit the onset of inhomogeneity occurs at leaner region, i.e. $\phi > 0.75$ for the

former and $\phi > 0.7$ for the latter. For the O₂ emissions, it is expected that O₂ level decreases with the increase of equivalence ratio, as the O₂ is consumed during reaction to convert into CO₂. The neat flame shows a linear reduction of O₂, of which diesel and NG show indistinguishable trend, while the PME flame shows slightly lower O₂ at $\phi > 0.75$.

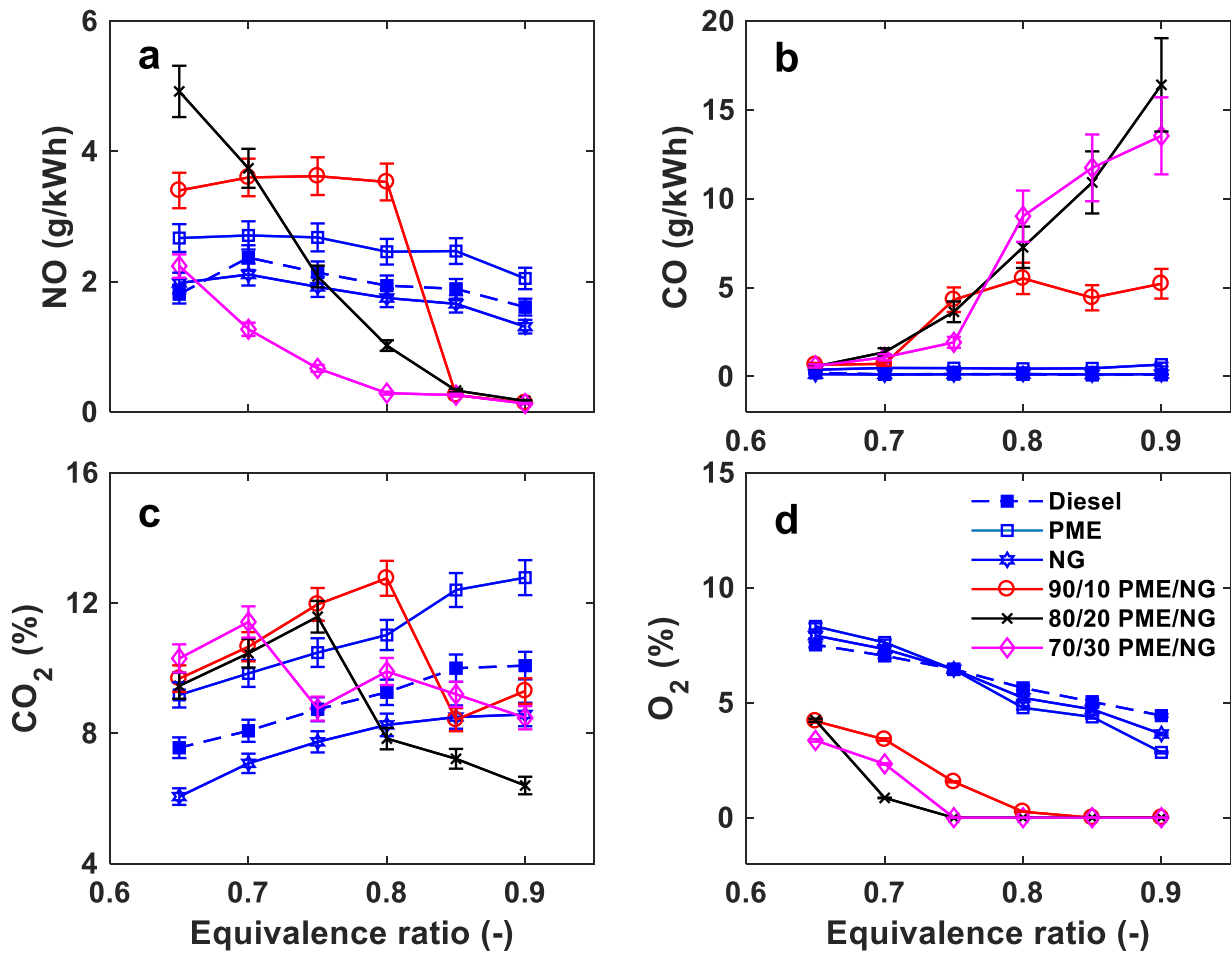


Fig. 6 Comparison of the emissions of (a) NO (b) CO (c) CO₂ and (d) O₂ for diesel, PME, 90/10, 80/20 and 70/30 PME/NG at ALR=2.5, preheated air temperature of 250 °C as a function of equivalence ratios.

Comparison of the emissions profiles between two equivalence ratios, $\phi=0.65$ and 0.9 is shown in Fig.7. It is evident that dual-fuel operation exhibits different emissions profiles compared to single liquid fuel flames. Variation of the fuel flow between primary main liquid fuel and secondary gaseous fuel results in the stratification of fuel/air mixture that leads to different emissions characteristics attributable to the changes in flow field, mixing and burning mode. For $\phi=0.9$, the NO emissions for diesel, PME and NG are significantly higher than dual-fuel cases, signifying better homogeneity in burning and higher flame temperature as a result of higher heat release. Although the dual-fuel flames are established based on two different streams of fuel flow, only one flame is seen to establish at the burner outlet, as shown in the flame images (Fig. 2). The secondary premixed NG and air is too weak to establish a flame. To a large extent the effectiveness of combustion for dual-fuel relies on the recirculation flow and turbulence in the combustor. The increasing CO emissions for higher NG fraction in the dual-fuel blends clearly indicates the incomplete combustion of fuels, as spots of fuels remains unreacted. The low NO for dual-fuel is indicative of low flame temperature, supported by the lower radical intensities shown in Fig. 5 due to lowly intense flame. It can be deduced that the strength of the central or corner recirculation flows is insufficient to recirculate the unburnt products back to the flame core for combustion, especially for $\phi=0.9$ where the swirling air portion is reduced. For $\phi=0.65$, the supplied main swirl air is about 45% more than $\phi=0.9$, hence the exit flow velocity is higher and a stronger toroidal strength can be generated to achieve better mixing. Fig. 7a shows that the NO emissions for dual-flame established at $\phi = 0.9$ are comparable with neat single flame, but the CO is still relatively higher, indicating a deficiency in mixing. However, comparing the actual values of CO between both equivalence ratios, implementing dual-fuel injection under ultra lean-burning condition seems a viable option to achieve a relatively low NO, but further optimisation of the injection system is needed to achieve both low NO and CO emissions. The CO₂ produced seems comparable between

dual-fuel with single neat fuels for both equivalence ratios, except that dual-fuel flames seem to emit slightly higher CO₂ level at $\phi=0.65$. The O₂ for dual-flames at $\phi=0.9$ is negligible, indicating the complete consumption of O₂ by the flames.

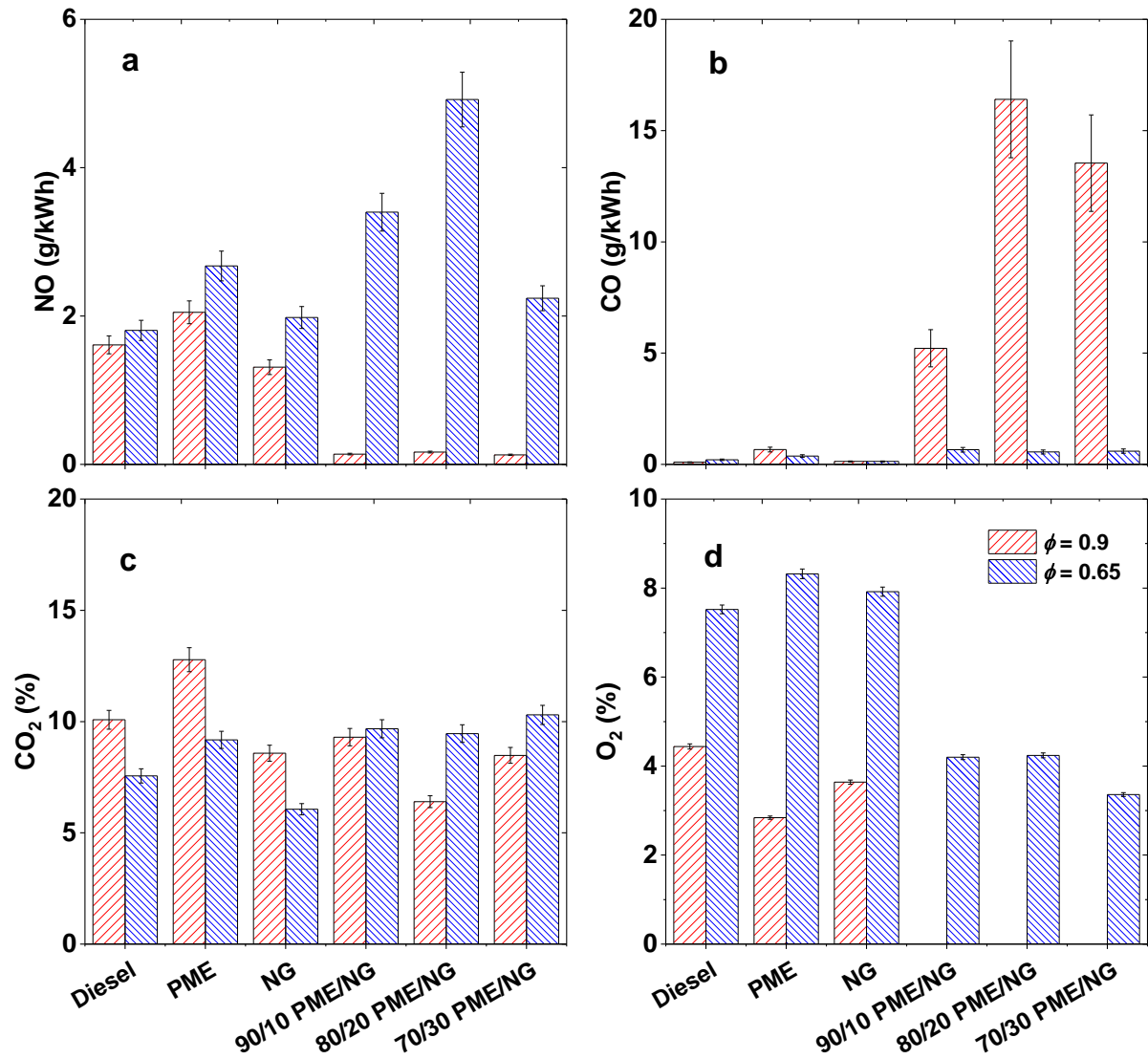


Fig. 7 Comparison of the (a) NO, (b) CO, (c) CO₂ and (d) O₂ emissions between global equivalence ratio of $\phi = 0.65$ and $\phi = 0.9$ for different single fuels and dual-fuel operations.

6.0 Conclusion

The combustion and emissions characteristics of dual-fuel operation using palm biodiesel and natural gas were investigated and compared against neat PME and diesel at constant thermal power of 9.3 kW using a swirl flame burner. The dual-fuel flame structures are rather similar to the neat PME flame, which are bluish in nature due to the usage of air-assisted atomiser. However, the flame structure is less well-defined as compared to the single-fuel flames with occasional flickers of sooty yellowish flames. Further investigation of the flame spectroscopic characteristic reveals that the main radicals such as OH*, CH*, CN* and C₂* radicals between the flames are different, which corresponds to the observed different flame intensities. The dual-flame exhibits lower CH* and OH* radical intensities compared to neat the PME fuel. There is no evidence of soot spectra from the dual-fuel flames, unlike those shown by diesel. Hence, the dual-flame exhibits the spectral characteristics of neat PME, albeit with lower radical intensity count as the flame intensity is reduced. The emissions performance for dual-fuel flames are compared against the single-fuel flames of PME, diesel and NG. Results show that dual-fuel operation of PME/NG produced inferior emissions performance, owing to the stratification of fuel/air mixture that contributes to the globally inhomogeneous mixing, subsequently leading to the ineffectiveness in combustion resulting in high CO and NO. However, a comparison of the flame emissions at $\phi = 0.65$ and $\phi = 0.9$ shows that the former produce comparable CO but higher NO than single fuel flames, while the latter produced comparatively lower NO but high CO. The underlying reasons for the varied emissions can be traced to flame temperature and turbulence level in the flow field. This work shows that optimisation of the fuel injection system and the combustor operating conditions is needed when switching from single fuel to dual-fuel operation in a swirl flame type burner, and that the strategy to achieve low emissions combustion is possible with the usage of biodiesel and natural gas.

References

- [1] Renewable Energy Policy Network for the 21st Century, Renewables 2017: Global Status Report, 2017.
- [2] M.C. Chiong, C.T. Chong, J.-H. Ng, S.S. Lam, M.-V. Tran, W.W.F. Chong, M.J. Mohammad Nazri, V.-M. Agustin, Liquid biofuels production and emissions performance in gas turbines : A review, *Energy Convers. Manag.* 173 (2018) 640–658.
- [3] IEA, Technology Roadmap: Delivering Sustainable Bioenergy, 2017.
- [4] M.Y.E. Selim, Pressure-time characteristics in diesel engine fueled with natural gas, *Renew. Energy.* 22 (2001) 473–489.
- [5] K. Wannatong, N. Akarapanyavit, S. Siengsanorh, S. Chanchaona, Combustion and knock characteristics of natural gas diesel dual fuel engine, *SAE Tech. Pap.* (2017) 2007–01–2047.
- [6] M.S. Lounici, K. Loubar, L. Tarabet, M. Balistrrou, D.C. Niculescu, M. Tazerout, Towards improvement of natural gas-diesel dual fuel mode: An experimental investigation on performance and exhaust emissions, *Energy.* 64 (2014) 200–211.
- [7] B. Yang, C. Xi, X. Wei, K. Zeng, M.C. Lai, Parametric investigation of natural gas port injection and diesel pilot injection on the combustion and emissions of a turbocharged common rail dual-fuel engine at low load, *Appl. Energy.* 143 (2015) 130–137.
- [8] B. Yang, X. Wei, C. Xi, Y. Liu, K. Zeng, M.C. Lai, Experimental study of the effects of natural gas injection timing on the combustion performance and emissions of a turbocharged common rail dual-fuel engine, *Energy Convers. Manag.* 87 (2014) 297–304.
- [9] L. Sun, Y. Liu, K. Zeng, R. Yang, Z. Hang, Combustion performance and stability of a dual-fuel diesel-natural-gas engine, *Proc. Inst. Mech. Eng. Part D J. Automob. Eng.* 229 (2015) 235–246.
- [10] R.G. Papagiannakis, D.T. Hountalas, Combustion and exhaust emission characteristics of a dual fuel compression ignition engine operated with pilot diesel fuel and natural gas, *Energy Convers. Manag.* 45 (2004) 2971–2987.
- [11] S.R. Krishnan, K.K. Srinivasan, S. Singh, S.R. Bell, K.C. Midkiff, W. Gong, S.B. Fiveland, M. Willi, Strategies for Reduced NO Emissions in Pilot-Ignited Natural Gas Engines, *J. Eng. Gas Turbines Power.* 126 (2004) 665.
- [12] M.A. Altaher, H. Li, G. Andrews, Co-firing of Kerosene and Biodiesel with Natural Gas in a Low NO_x Radial Swirl Combustor, in: *Proc. ASME Turbo Expo 2012*, ASME (GT2012-68597), Copenhagen, Denmark, 2012.
- [13] H. Kurji, A. Valera-Medina, A. Okon, C.T. Chong, Combustion and emission performance of CO₂/CH₄/biodiesel and CO₂/CH₄/diesel blends in a Swirl Burner Generator, *Energy Procedia.* 142 (2017) 154–159.
- [14] L. Jiang, A.K. Agrawal, Combustion of straight glycerol with / without methane using a fuel-flexible , low-emissions burner, *Fuel.* 136 (2014) 177–184.
- [15] P. Queiros, M. Costa, R.H. Carvalho, Co-combustion of crude glycerin with natural gas and hydrogen, *Proc. Combust. Inst.* 34 (2013) 2759–2767.
- [16] E.R. Jayaratne, Z.D. Ristovski, L. Morawska, N.K. Meyer, Carbon dioxide emissions from diesel and compressed natural gas buses during acceleration, *Transp. Res. Part D Transp. Environ.* 15 (2010) 247–253.
- [17] P. Breeze, Gas-Turbine Power Generation, in: *Power Gener. Technol.*, Elsevier, 2005: pp. 43–61.
- [18] C.T. Chong, S. Hochgreb, Effect of Atomizing Air Flow on Spray Atomization of an Internal-Mix Twin-Fluid Atomizer, *At. Sprays.* 25 (2015) 657–673.

- [19] M.C. Chiong, C.T. Chong, J.H. Ng, M.V. Tran, S.S. Lam, A. Valera-Medina, M.N. Mohd Jaafar, Combustion and emission performances of coconut, palm and soybean methyl esters under reacting spray flame conditions, *J. Energy Inst.* 92 (2019) 1034–1044.
- [20] C.T. Chong, J.-H. Ng, M.S. Aris, G.R. Mong, N. Shahril, S.T. Ting, M.F. Zulkifli, Impact of gas composition variations on flame blowout and spectroscopic characteristics of lean premixed swirl flames, *Process Saf. Environ. Prot.* 128 (2019) 1–13.
- [21] T. Korakianitis, A.M. Namasivayam, R.J. Crookes, Diesel and rapeseed methyl ester (RME) pilot fuels for hydrogen and natural gas dual-fuel combustion in compression-ignition engines, *Fuel*. 90 (2011) 2384–2395.
- [22] S.K. Hoekman, A. Broch, C. Robbins, E. Cenicerros, M. Natarajan, Review of biodiesel composition, properties, and specifications, *Renew. Sustain. Energy Rev.* 16 (2012) 143–169.
- [23] C.T. Chong, S. Hochgreb, Spray combustion characteristics of palm biodiesel, *Combust. Sci. Technol.* 184 (2012) 1093–1107.
- [24] J. Schobing, V. Tschamber, A. Brillard, G. Leyssens, E. Iojoiu, V. Lauga, Impact of engine operating cycle, biodiesel blends and fuel impurities on soot production and soot characteristics, *Combust. Flame*. 198 (2018) 1–13.
doi:10.1016/J.COMBUSTFLAME.2018.08.025.
- [25] R.G. Joklik, J.W. Daily, W.J. Pitz, Measurements of CH radical concentrations in an acetylene/oxygen flame and comparisons to modeling calculations, *Symp. Combust.* 21 (1988) 895–904.
- [26] D. Zhao, H. Yamashita, K. Kitagawa, N. Arai, T. Furuhashi, Behavior and effect on NO_x formation of OH radical in methane-air diffusion flame with steam addition, *Combust. Flame*. 44 (2003) 98–99.
- [27] R.M.I. Elsamra, S. Vranckx, S.A. Carl, CH(A₂) formation in hydrocarbon combustion: The temperature dependence of the rate constant of the reaction C₂H + O₂ → CH(A₂) + CO₂, *J. Phys. Chem. A*. 109 (2005) 10287–10293.
- [28] W. Juchmann, H. Latzel, D.I. Shin, G. Peiter, T. Dreier, H.-R. Volpp, J. Wolfrum, R.P. Lindstedt, K.M. Leung, Absolute Radical Concentration Measurements and Modeling of Low-Pressure CH₄/O₂/NO Flames, *Proc. Combust. Inst.* 27 (1998) 469–476.
- [29] J. Kojima, Y. Ikeda, T. Nakajima, Basic aspects of OH(A), CH(A), and C₂(d) chemiluminescence in the reaction zone of laminar methane-air premixed flames, *Combust. Flame*. 140 (2005) 34–45.
- [30] S.R. Turns, *An introduction to combustion: concepts and applications*, 3rd ed., McGrawHill, 2012.
- [31] C.T. Chong, S. Hochgreb, Spray flame structure of rapeseed biodiesel and Jet-A1 fuel, *Fuel*. 115 (2014) 551–558.
- [32] C.T. Chong, S. Hochgreb, Flame structure, spectroscopy and emissions quantification of rapeseed biodiesel under model gas turbine conditions, *Appl. Energy*. 185 (2017) 1383–1392.
- [33] B. Higgins, M.Q. Mcquay, F. Lacas, S. Candel, An experimental study on the effect of pressure and strain rate on CH chemiluminescence of premixed fuel-lean methane/air flames, *Fuel*. 80 (2001) 1583–1591.
- [34] B. Higgins, M.Q. Mcquay, F. Lacas, J.C. Rolon, N. Darabiha, S. Candel, Systematic measurements of OH chemiluminescence for fuel-lean, high-pressure, premixed, laminar flames, *Fuel*. 80 (2001) 67–74.
- [35] C.K. Law, *Combustion Physics*, Cambridge University Press, 2006.
- [36] H. Kahila, A. Wehrfritz, O. Kaario, V. Vuorinen, Large-eddy simulation of dual-fuel

- ignition : diesel spray injection into a lean methane-air mixture, *Combust. Flame.* 199 (2019) 131–151.
- [37] G.P. Smith, J. Luque, C. Park, J.B. Jeffries, D.R. Crosley, Low pressure flame determinations of rate constants for OH(A) and CH(A) chemiluminescence, *Combust. Flame.* 131 (2002) 59–69.
- [38] J. Giménez-López, A. Millera, R. Bilbao, M.U. Alzueta, HCN* oxidation in an O₂/CO₂ atmosphere: An experimental and kinetic modeling study, *Combust. Flame.* 157 (2010) 267–276.
- [39] R.A. Perry, C.F. Melius, The Rate and Mechanism of the Reaction of HCN with Oxygen Atoms the Temperature Range 540-900 K *, *Symp. Combust.* 20 (1984) 639–646.